Title: Structural study and crystallization behaviour of Fe62-xCoxNb8B30 metallic glasses (x = 0, 20)

Author: R. Babilas, Mariola Kądziołka-Gaweł

Citation style: Babilas R., Kądziołka-Gaweł Mariola. (2016). Structural study and crystallization behaviour of Fe62-xCoxNb8B30 metallic glasses (x = 0, 20). "Acta Physica Polonica. A" (Vol. 130, nr 4 (2016), s. 901-904), doi 10.12693/APhysPolA.130.901

Proceedings of the XXIII Conference on Applied Crystallography, Krynica Zdrój, Poland, September 20–24, 2015

Structural Study and Crystallization Behaviour of $Fe_{62-x}Co_xNb_8B_{30}$ Metallic Glasses ($x = 0,\ 20$)

R. Babilas[a,*] and M. Kądziołka-Gaweł[b]

[a]Institute of Engineering Materials and Biomaterials, Silesian University of Technology, S. Konarskiego 18a, 44-100 Gliwice, Poland

[b]Institute of Physics, University of Silesia, Uniwersytecka 4, 40-007 Katowice, Poland

The paper presents the structural analysis of $Fe_{62-x}Co_xNb_8B_{30}$ metallic glasses ($x = 0,\ 20$) in as-cast and after crystallization state. The studies were performed on metallic glasses of ribbon form with thickness of 0.05 and 0.06 mm. The structure analysis of the samples in as-cast state and phase analysis of studied alloys after annealing was carried out by the X-ray diffraction methods. Moreover, the Mössbauer spectroscopy was also used to investigate the local structure for examined alloys. The soft magnetic properties examination covered the initial magnetic permeability. The after-effects of magnetic permeability were also conducted.

DOI: 10.12693/APhysPolA.130.901

PACS/topics: 61.05.cp, 64.70.pe, 75.50.Bb, 75.50.Kj

1. Introduction

The Fe-based glassy alloys received great attention of researchers, because of their good physical properties [1]. The work succeeded in preparation of ternary and quaternary Fe-based metallic glasses, which are potential candidates for soft magnetic materials.

Gersci et al. [2] succeeded to prepare $(Fe_{1-x}Co_x)_{62}Nb_8B_{30}$ glassy alloys with $x = 0,\ 0.33,$ and 0.50. They studied the electric and magnetic properties of rapidly quenched samples in the form of ribbons with thickness of 0.035 mm. Authors revealed that Co addition caused a decrease of the magnetostriction coefficient and led to the change in a shape of the hysteresis loops.

Basing on [2], the aim of the paper is the structure analysis of $Fe_{62-x}Co_xNb_8B_{30}$ ($x = 0,\ 20$) metallic glasses in as-cast and after annealing state using the X-ray diffraction and Mössbauer spectroscopy. The Mössbauer spectroscopy was chosen as a suitable technique to detect the nearest neighbours of the resonant Fe atoms.

2. Experimental

The studies were performed on $Fe_{62}Nb_8B_{30}$ and $Fe_{42}Co_{20}Nb_8B_{30}$ metallic glasses in the form of ribbons with the thickness of 0.05 and 0.06 mm and the width of 5 mm. The ingots of alloys were prepared by induction heating a mixture of all pure elements together: Fe (99.98%), Co (99.99%), B (99.9%), Nb (99.95%) in nominal compositions. The amorphous ribbons were prepared by the melt spinning technique [3, 4]. The casting conditions included a linear speed of Cu wheel of 20 m/s and ejection over-pressure of molten alloy under Ar of 0.03 MPa.

The structure of the samples in as-cast state was examined by X-ray diffraction (XRD) in reflection mode using the diffractometer with Cu K_α radiation. For the samples after crystallization measurements were done with using Co K_α radiation. The diffraction patterns for all samples were collected by "step-scanning" method in the 2θ range from 30° to 90°.

The ^{57}Fe Mössbauer spectra were recorded at room temperature using a constant acceleration spectrometer with triangular velocity shape, a multichannel analyzer with 1024 channels, and linear arrangement of the ^{57}Co(Cr) source (≈15 mCi), absorber and detector. The spectrometer velocity was calibrated with a high purity α-Fe foil. The Mössbauer spectra determined after annealing were calculated by means of a discrete analysis (a few Zeeman sextets). All spectra were fitted by means of a hyperfine field distribution using the Hesse–Rübartsch procedure with linear correlation between isomer shift and hyperfine magnetic field [5].

Magnetic measurements of as-cast ribbons, carried out at room temperature, included relative magnetic permeability (μ_r) and disaccommodation of magnetic permeability ($\Delta\mu/\mu$) and were determined by the LCR Meter at a frequency of 1030 Hz and magnetic field up to 100 A/m. $\Delta\mu/\mu$ also known as the after-effects of magnetic permeability was determined by measuring changes of magnetic permeability (μ) as a function of time (t) after demagnetization, where $\Delta\mu$ is difference between magnetic permeability determined at $t_1 = 30$ s and $t_2 = 1800$ s after demagnetization and μ at t_1.

3. Results and discussion

Figure 1 shows the XRD patterns of the melt-spun $Fe_{62-x}Co_xB_{30}Nb_8$ ($x = 0,\ 20$) alloys. No appreciable diffraction peaks corresponding to crystalline phases were detected. Only broad peaks were observed, which implies the formation of Fe-based amorphous structure.

*corresponding author; e-mail: rafal.babilas@polsl.pl

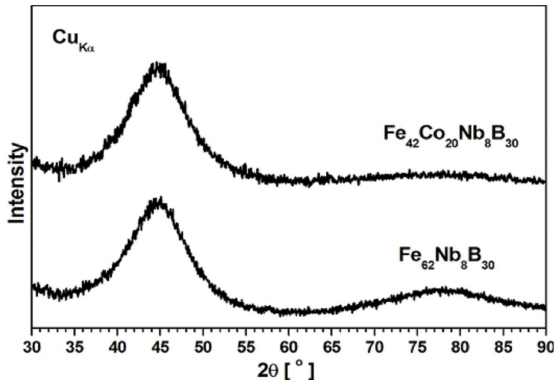

Fig. 1. X-ray diffraction patterns of $Fe_{62-x}Co_xNb_8B_{30}$ alloys in as-cast state.

The room temperature Mössbauer spectra obtained for alloys in as-cast state are shown in Fig. 2. The spectra present broadened sextet patterns typical for the structural disorder of amorphous ferromagnetic alloys. The corresponding hyperfine magnetic fields distributions $p(B_{\rm hf})$ for glassy alloys are also presented in Fig. 3. Several local picks or swells can be distinguished in the $p(B_{\rm hf})$ distributions of reflecting preferential surrounding of iron atoms. The hyperfine magnetic fields distributions were also decomposed into low and high field components by Gaussian distributions. For $Fe_{62}Nb_8B_{30}$ alloy two positions are visible at about 8.6 T and main maximum at about 18.9 T. Replacing Fe atoms by Co addition caused changes in local neighborhood of iron which leads to change in $p(B_{\rm hf})$ and three swells can be visible (positioned at about: 3.9, 10.5, and 17.8 T). The presence of smaller peaks at low hyperfine field values in the range from 3 to 15 T for the as-cast samples can be ascribed to the presence of nonferromagnetic atoms of Nb in the neighborhood of Fe atoms, as it was reported in [6, 7], as no evidence of such low values in Fe–Co–Nb–B amorphous alloys.

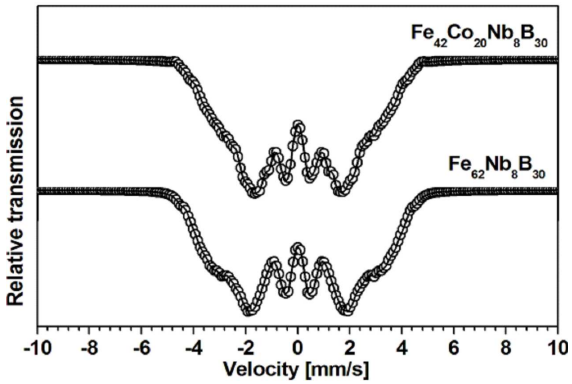

Fig. 2. Mössbauer spectra of studied alloys in as-cast state.

The mean values of the hyperfine magnetic field ($B_{\rm hf}$) as well as the isomer shift (IS) parameters obtained from $p(B_{\rm hf})$ for the best fitting are listed in Table I. The addition of Fe atoms by Co lead to changes in hyperfine magnetic field distributions and an average values of IS. For $Fe_{42}Co_{20}Nb_8B_{30}$ a value of $B_{\rm hf}$ is lower but the IS parameter is higher in a comparison with the same parameters determined for the ternary alloy without Co. A strong modification of electronic structure by Co addition can be suggested. Moreover, an existence of nonmagnetic regions which do not comprise Fe and consequently are not detected with the Mössbauer spectroscopy can be also considered.

Table I gives also information about the initial ($\mu_{\rm r}$) and the intensity of disaccommodation of magnetic permeability ($\Delta\mu/\mu$). Allia and Vinai [8] stated that the intensity of $\Delta\mu/\mu$ (magnetic after-effects) is directly proportional to the concentration of free volume in glassy materials, which is formed during cooling of molten alloy. The $\Delta\mu/\mu$ reached a value of 11.7% for $Fe_{62}Nb_8B_{30}$ (0.05 mm) and 8.1% for $Fe_{42}Co_{20}Nb_8B_{30}$ (0.06 mm) ribbons, adequately. These results mean that higher concentration of free volume is formed in ribbons with lower thickness.

TABLE I

Average values of IS, $B_{\rm hf}$, initial magnetic permeability ($\mu_{\rm r}$) and disaccommodation of magnetic permeability ($\Delta\mu/\mu$) of $Fe_{62-x}Co_xNb_8B_{30}$ metallic glasses in as-cast state.

Glassy alloy	IS [mm/s]	$B_{\rm hf}$ [T]	$\mu_{\rm r}$	$\Delta\mu/\mu$ [%]
$Fe_{62}Nb_8B_{30}$	0.095	17.0	267	11.7
$Fe_{42}Co_{20}Nb_8B_{30}$	0.127	15.3	291	8.1

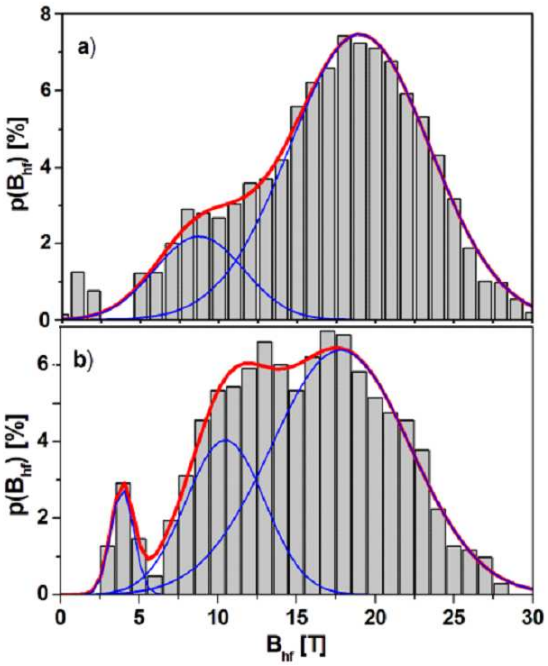

Fig. 3. Hyperfine magnetic field distribution of: (a) $Fe_{62}Nb_8B_{30}$ and (b) $Fe_{42}Co_{20}Nb_8B_{30}$ metallic glasses with its deconvolution into low and high field components.

Furthermore, Allia and Vinai also stated that there is a connection between the magnetic after-effects and structural disorder of selected ferromagnetic metallic glasses. The $\Delta\mu/\mu$ is sensitive to the short-range order of atoms. Therefore, the variation of the average hyperfine magnetic field with Co addition could be connected with topological and chemical disorder of the studied glassy samples.

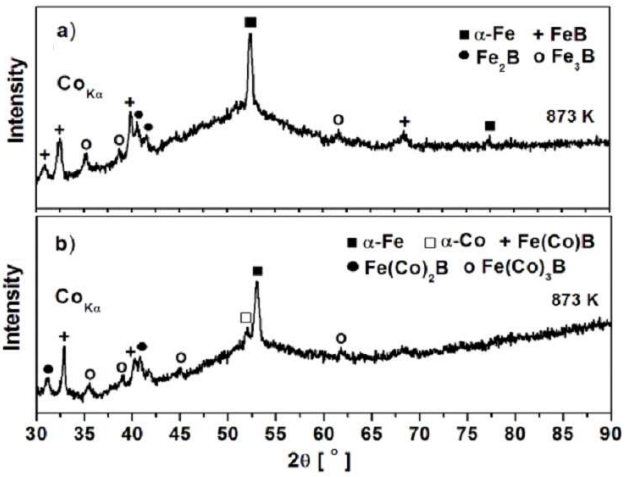

Fig. 4. X-ray diffraction patterns of: (a) $Fe_{62}Nb_8B_{30}$ and (b) $Fe_{42}Co_{20}Nb_8B_{30}$ alloys after annealing at 873 K/1 h.

Figure 4 shows XRD patterns obtained for alloys after annealing for 1 h at 873 K. Qualitative phase analysis from X-ray data enables the identification of α-Fe phase and iron borides — FeB, Fe_2B, Fe_3B for ribbons of $Fe_{62}Nb_8B_{30}$ alloy. The annealing of quaternary alloy with Co addition obviously caused a formation of crystalline α-Fe(Co) and iron, cobalt borides — Fe(Co)B, $Fe(Co)_2B$, and $Fe(Co)_3B$.

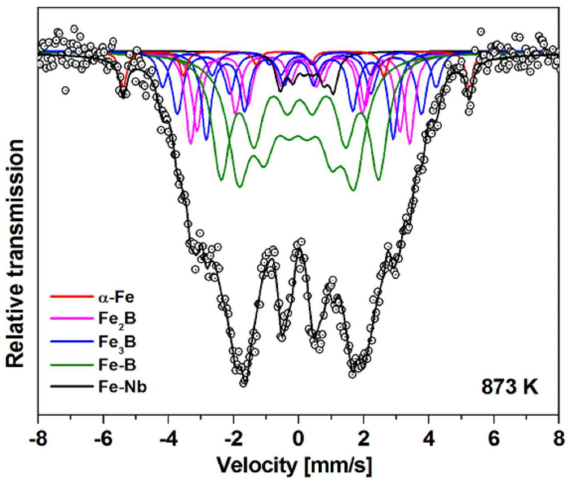

Fig. 5. Transmission Mössbauer spectrum and fittings of $Fe_{62}Nb_8B_{30}$ metallic glass after annealing at 873 K/1 h.

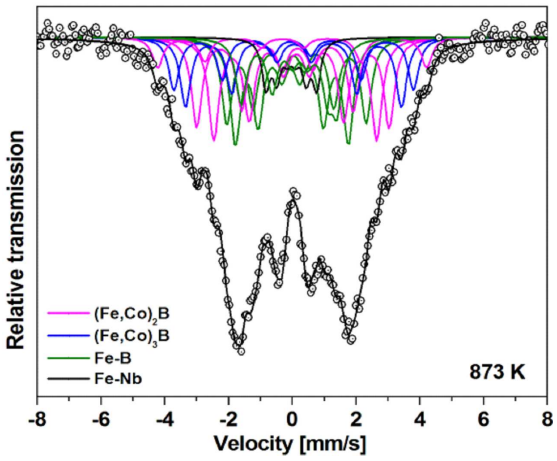

Fig. 6. As in Fig. 5 but for $Fe_{42}Co_{20}Nb_8B_{30}$ metallic glass.

TABLE II

Hyperfine parameters of alloys annealed at 873 K/1h (A — relative area from the spectra). Experimental errors are smaller than 5%.

Glassy alloy	IS [mm/s]	B_{hf} [T]	A [%]	Phase
$Fe_{62}Nb_8B_{30}$	0.325	5.1	4	Fe–Nb
	0.009	11.1	28	Fe–B
	0.090	15.1	24	Fe–B
	0.172	19.4	17	Fe_2B
	0.088	23.4		
	0.073	17.9	24	Fe_3B
	0.080	20.9		
	–0.046	26.2		
	–0.210	33.0	3	α–Fe
$Fe_{42}Co_{20}Nb_8B_{30}$	0.027	5.0	6	Fe-Nb
	0.128	9.3	10	Fe–Nb
	0.028	11.0	16	Fe–B
	0.142	13.6	13	Fe–B
	0.107	21.0	19	$(Fe,Co)_2B$
	0.072	23.4		
	0.169	15.9	35	$(Fe,Co)_3B$
	0.150	18.7		
	–0.095	26.2		

The room temperature Mössbauer spectra determined after annealing are shown in Fig. 5, 6. The fitting parameters of these spectra and the assigned phases are reported in Table 2. In comparison with that of as-cast samples, one can observe a refinement of external lines, while the central part of the spectra remains almost unresolved. This evolution could be interpreted by the presence of both well crystallized grains and a residual disordered amorphous matrix. The experimental spectrum of annealed $Fe_{62}Nb_8B_{30}$ alloy was fitted with nine sextets, hyperfine parameters two of them corresponding to Fe_2B [9], three to Fe_3B [10, 11] and one to α-Fe. The other sextets are connected with remainder of amorphous phase.

What is more, the spectrum obtained for $Fe_{42}Co_{20}Nb_8B_{30}$ was also fitted with nine sextets, which include two sextets for $Fe(Co)_2B$ and three for $Fe(Co)_3B$. It is not observed the hyperfine field values higher 33 T indicative of existence of crystalline phase connected with pure Fe or Fe-Co [12, 13].

4. Conclusions

Substitution of Fe atoms by Co led to change of hyperfine magnetic fields (B_{hf}) distributions and an average values of isomer shift (*IS*). The Co addition caused changes in local neighborhood of iron what lead to changing in $p(B_{hf})$ and three swells can be visible. The presence of smaller peaks at low hyperfine field values in the range from 3 to 15 T can be probably related to the presence of nonferromagnetic atoms of Nb in the neighborhood of Fe atoms. The variation of the average hyperfine magnetic field with Co addition could be also connected with the intensity of $\Delta\mu/\mu$ (magnetic after-effects), which is sensitive to the short-range order of atoms.

What is more, addition of this element also caused the improve of magnetic permeability and induced formation of crystalline phases including the α-Fe(Co), $(Fe,Co)_2B$ and $(Fe,Co)_3B$ after annealing at 873 K/1 h.

Combination of X-ray diffraction, Mössbauer spectroscopy and magnetic permeability measurements seems to be very helpful approach for examining the structural environment of Fe atoms on a short-range ordering scale and also analysis of crystalline phases.

Acknowledgments

The work was supported by National Science Centre under research project no. 2011/03/D/ST8/04138.

References

[1] A. Inoue, *Mater. Sci. Eng. A* **304–306**, 1 (2001).

[2] Zs. Gercsi, F. Mazaleyrat, S.N. Kane, L.K. Varga, *Mater. Sci. Eng. A* **375–377**, 1048 (2004).

[3] R. Babilas, M. Kądziołka-Gaweł, *Acta Phys. Pol. A* **127**, 573 (2015).

[4] R. Babilas, Ł. Hawełek, A. Burian, *J. Solid State Chem.* **219**, 179 (2014).

[5] J. Frąckowiak, *Hyperfine Interact.* **54**, 793 (1990).

[6] J.S. Blazquez, J.M. Borrego, C.F. Conde, A. Conde, J.M. Greneche, *J. Phys. Condens. Matter* **15**, 3957 (2003).

[7] A. Charris Hernandez, Z. Caamano De Avila, G.A. Perez Alcazar, *Rev. Mex. Fis. S* **58**, 52 (2012).

[8] P. Allia, F. Vinai, *Phys. Rev. B* **33**, 422 (1986).

[9] J. Torrens-Serra, P. Bruna, J. Rodriguez-Viejo, T. Pradell, *Rev. Adv. Mater. Sci.* **18**, 464 (2008).

[10] M. Arshed, M. Siddique, M. Anwar-ul-Islam, A. Ashfag, A. Shamim, N.M. Butt, *Solid State Commun.* **98**, 427 (1996).

[11] M. Yamasaki, M. Hamano, T. Kobayashi, *Mater. Trans.* **43**, 2885 (2002).

[12] R. Bruning, K. Samwer, C. Kuhrt, L. Schultz, *J. Appl. Phys.* **72**, 2978 (1992).

[13] N.S. Cohen, Q.A. Pankhurst, L.F. Barquin, *J. Phys. Condens. Matter* **11**, 8839 (1999).